



# Chapter 57

## Quantitative Visualization of Sub-Micron Deformations and Stresses at Sub-Microsecond Intervals in Soda-Lime Glass Plates

Chengyun Miao and Hareesh V. Tippur

**Abstract** Full-field optical measurement of deformations and stresses on transparent brittle ceramics such as soda-lime glass is rather challenging due to the low toughness and high stiffness characteristics. Particularly, the surface topography and stress field evaluation from measured orthogonal surface slopes and stress gradients could be of considerable significance for visualizing and quantifying deformation of glass plates under dynamic impact loading. In this work, two full-field optical techniques, reflection Digital Gradient Sensing (or r-DGS) and a new DGS method, called transmission-reflection Digital Gradient Sensing (or tr-DGS) are employed to quantify surface slopes and stress gradients, respectively, as glass specimens are subjected dynamic impact loading using a modified Hopkinson pressure bar. These two methods can measure extremely small angular deflections of light rays caused by surface deformations and local stresses in specimens. The tr-DGS methodology is especially more sensitive than r-DGS. Using such optical methods, sub-micron surface deflections and the corresponding stress field,  $(\sigma_{xx} + \sigma_{yy})$ , can be quantified using a Higher-order Finite-difference-based Least-squares Integration (HFLI) scheme. When used in conjunction with ultrahigh-speed photography, microsecond or sub-microsecond temporal resolution is possible.

**Keywords** Digital gradient sensing · Dynamic impact loading · Transparent brittle ceramics · Deflections and stresses · Ultrahigh-speed photography

### 57.1 Introduction

Transparent ceramics such as soda-lime glass is popular engineering material as it offers benefits such as high stiffness and hardness, and very high compression strength besides low cost and high sustainability. Further, polymer-laminated glasses are used as transparent armor in military applications. The ability to bear load under dynamic impact is critical as well. Hence, quantitative visualization of deformations under dynamic impact loading is important.

A few years ago Periasamy and Tippur [1] proposed a full-field optical method called Digital Gradient Sensing (DGS) for measuring two orthogonal in-plane stress gradients in transparent solids. It employs 2D DIC for quantifying elasto-optic effects in transparent materials. Subsequently, they [2] extended DGS to study reflective objects by measuring two orthogonal surface slopes. The simplicity of the experimental setup, good accuracy, and easy access to image correlation algorithms make DGS very attractive for experimental mechanics investigations. Furthermore, these measured quantities can be numerically integrated readily to evaluate surface topography or stress fields. Miao et al. investigated the feasibility of r-DGS in conjunction with a robust Higher-order Finite-difference-based Least-squares Integration (or simply HFLI) scheme to measure the surface topography of thin structures [3, 4]. Later on, the authors showed that r-DGS can be used with HFLI to measure sub-micron deformations at microsecond resolution on composite plates under dynamic loading [5]. Very recently, the authors proposed two modified DGS variants with even higher measurement sensitivity [6], which are valuable for studying high stiffness and low toughness materials such as glass. Sundaram and Tippur have applied transmission-mode DGS (t-DGS) to study dynamic fracture mechanics of transparent and brittle materials including glass [7–12]. Considering their work, the feasibility of other DGS methods being applied to study glass needs to be examined. In this context, sub-micron deformations in glass plates are measured at sub-microsecond intervals and stresses are evaluated in glass plate.

---

C. Miao · H. V. Tippur (✉)  
Department of Mechanical Engineering, Auburn University, Auburn, AL, USA  
e-mail: [htippur@eng.auburn.edu](mailto:htippur@eng.auburn.edu)

## 57.2 Experimental Details

### 57.2.1 Reflection-Mode Digital Gradient Sensing (r-DGS)

A schematic of the experimental setup for reflection-mode Digital Gradient Sensing (or r-DGS) to measure surface slopes is shown in Fig. 57.1. A digital camera is used to record random speckles on a target plane via the reflective specimen surface. To achieve this, the specimen and the target plate are placed perpendicular to each other, and the beam splitter is placed at 45° relative to the specimen and target plate, respectively. The target plate is coated with random black and white spray painted speckles, and is illuminated uniformly using ordinary white light.

For simplicity, the angular deflections of light rays only in the  $y$ - $z$  plane are shown in Fig. 57.2. When the specimen is in the undeformed state, a point P on the target plate comes into focus through point O on the specimen surface. The speckle image is recorded at this instant as the reference image. After the specimen suffers out-of-plane deformation due to the impact load, a neighboring point Q on the target plate comes into focus through the same point on the specimen surface O. The corresponding deformed image is recorded next. The local displacements  $\delta_{y:x}$  can be obtained by performing a 2D image correlation of the reference and deformed images. OP makes an angle  $\phi_y$  with OQ and  $\phi_y = \theta_i + \theta_r$  where  $\theta_r$  ( $=\theta_i$ ) are incident and reflected angles relative to the normal to the specimen. The two orthogonal surface slopes can be expressed as  $\frac{\partial w}{\partial y:x} = \frac{1}{2} \tan(\phi_{y:x})$ . The governing equations for r-DGS are [2]:

$$\frac{\partial w}{\partial y:x} = \frac{1}{2} \tan(\phi_{y:x}) \approx \frac{1}{2} (\phi_{y:x}) \approx \frac{1}{2} \left( \frac{\delta_{y:x}}{\Delta} \right), \quad (57.1)$$

where  $\Delta$  is the distance between the specimen and target plate. The details of the specimen surface for r-DGS are shown in Fig. 57.3a. The specimen surface is made reflective using vapor deposition of aluminum film. (The front face of the specimens illustrated in Fig. 57.3 is towards to the camera and the target plate.)

### 57.2.2 Transmission-Reflection Digital Gradient Sensing (tr-DGS)

The schematic of the experimental setup for transmission-reflection Digital Gradient Sensing (tr-DGS) method is similar to the one shown in Fig. 57.1. However, in tr-DGS, the specimen is transparent but its rear face is made reflective by a reflective

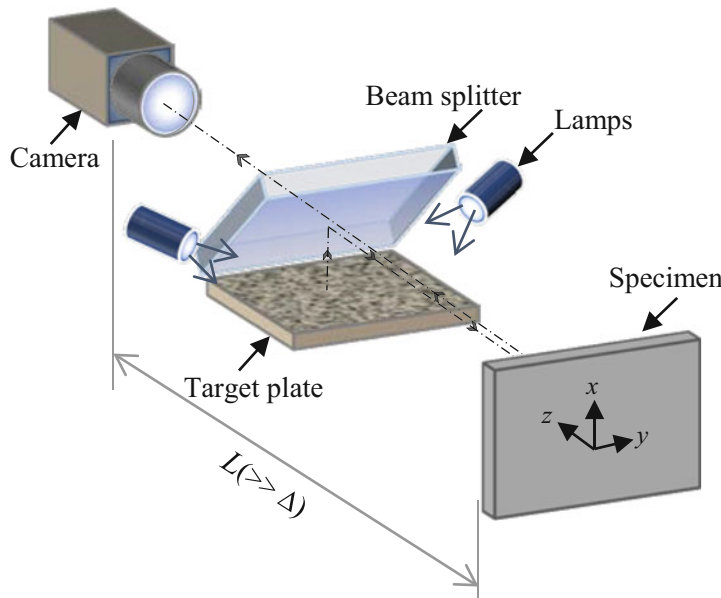


Fig. 57.1 Schematic of experimental setup for r-DGS and tr-DGS methods [6]

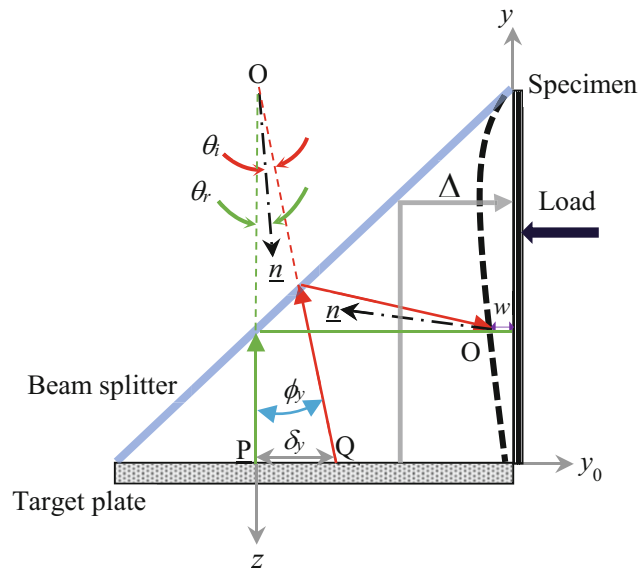


Fig. 57.2 Working principle of r-DGS [3]

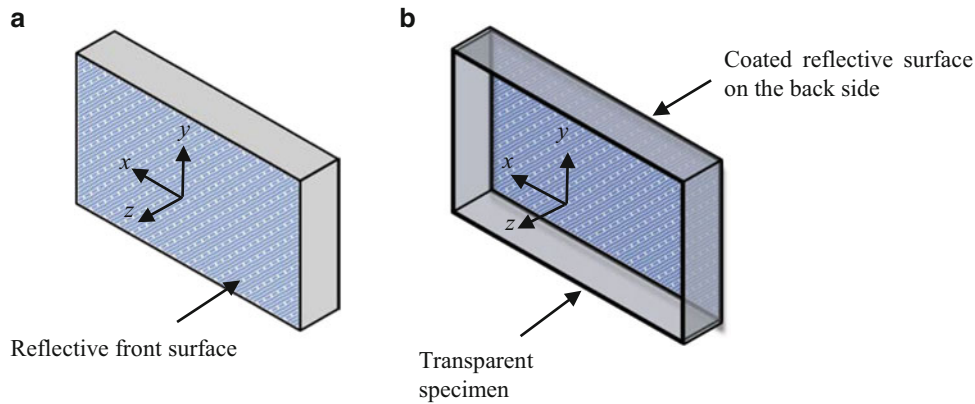


Fig. 57.3 Specimen configurations for: (a) r-DGS; (b) tr-DGS [5]

film deposition, as shown in Fig. 57.3b. The light rays from the target plate pass through the transparent specimen and reach the reflective surface. Then, they are reflected back by the reflective surface and pass through the transparent specimen again. As in r-DGS, a reference image is recorded first and then the deformed images as the specimen is subjected to load. The local displacements can be measured by correlating the reference image with the deformed images.

In r-DGS, the reflective surface deforms when the specimen suffers impact load. In tr-DGS, when the specimen is impacted, the refractive index and thickness of the specimen change; furthermore, the reflective rear surface also deforms. Hence, tr-DGS is much more sensitive than r-DGS. The two angular deflections of light rays of tr-DGS  $(\phi_{x:y})_{tr-DGS}$ , which are related to the in-plane stress gradients, can be expressed as [5],

$$(\phi_{x:y})_{tr-DGS} = \frac{\delta_{x:y}}{\Delta} = \left( 2C_{\sigma} B - \frac{\nu B}{E} \right) \frac{\partial (\sigma_{xx} + \sigma_{yy})}{\partial (x : y)}. \tag{57.2}$$

### 57.3 Glass Plate Subjected to Dynamic Impact

#### 57.3.1 Quantitative Evaluation of Sub-Micron Magnitude Deformations

The dynamic backside/lateral impact of soda-lime glass plate was studied using r-DGS in conjunction with ultrahigh-speed digital photography. The specimen was  $152.4 \text{ mm} \times 101.6 \text{ mm} \times 4.6 \text{ mm}$ . One of the two  $152.4 \times 101.6 \text{ mm}^2$  faces of the specimen was made reflective by depositing with a thin aluminum film. The reflective surface faces the target plate and the camera.

The schematic of the experimental setup employed is shown in Fig. 57.4. A modified Hopkinson pressure bar (or simply a 'long-bar') was used for loading the uncoated backside of the specimen. It included a 1.83 m steel rod of 25.4 mm diameter with a tapered end of 3 mm diameter impacting the backside of the specimen. A 305 mm long, 25.4 mm diameter steel striker was placed in the gas-gun barrel to impact the long-bar. The striker was launched towards the long-bar at a velocity of  $\sim 2.5 \text{ m/s}$  during the tests. At the same time, a Kirana-05 M ultrahigh-speed camera was used to record speckles on the target plane at 1.25 million frames per second (inter-frame period of  $0.8 \mu\text{s}$ ) in this experiment. The distance between the specimen and the camera lens plane ( $L$ ) was  $\sim 950 \text{ mm}$  and the one between the specimen mid-plane and the target plane ( $\Delta$ ) was 102 mm.

The time-resolved orthogonal surface slope contours  $\frac{\partial w}{\partial x}$  and  $\frac{\partial w}{\partial y}$  due to transient stress wave propagation in the glass plate are shown in the first two rows of Fig. 57.5 at a few select time instants. The start of the impact is at  $t = 0 \mu\text{s}$ . In the early stages of impact, deformations are concentrated close to the center of the plate resulting in sparse surface slope contours. With the passage of time, the contours get denser and larger with a higher concentration of contours near the contact point. The reconstructed 3D surfaces computed through 2D integration by using surface slope data from r-DGS in conjunction with HFLI are plotted in row 3 of Fig. 57.5. The out-of-plane deformation is around  $0.63 \mu\text{m}$  at  $t = 4 \mu\text{s}$ , which shows that this method is able to detect sub-micron deformations at sub-microsecond intervals.

#### 57.3.2 Quantification of Stress Fields

Quantitative evaluation of stress fields in soda-lime glass plate subjected to dynamic lateral impact was studied using tr-DGS in conjunction with ultrahigh-speed digital photography. The specimen was  $76 \text{ mm} \times 24 \text{ mm} \times 5.6 \text{ mm}$  strip with one of the two  $76 \times 5.6 \text{ mm}^2$  faces made reflective by depositing a thin aluminum film. The non-reflective surface of the glass strip faces the camera.

The schematic of the experimental setup for this experiment is similar to the previous one. A long-bar was used for impact loading the  $24 \text{ mm} \times 5.6 \text{ mm}$  face of the specimen using a 1.83 m steel rod of 25.4 mm diameter with a tapered

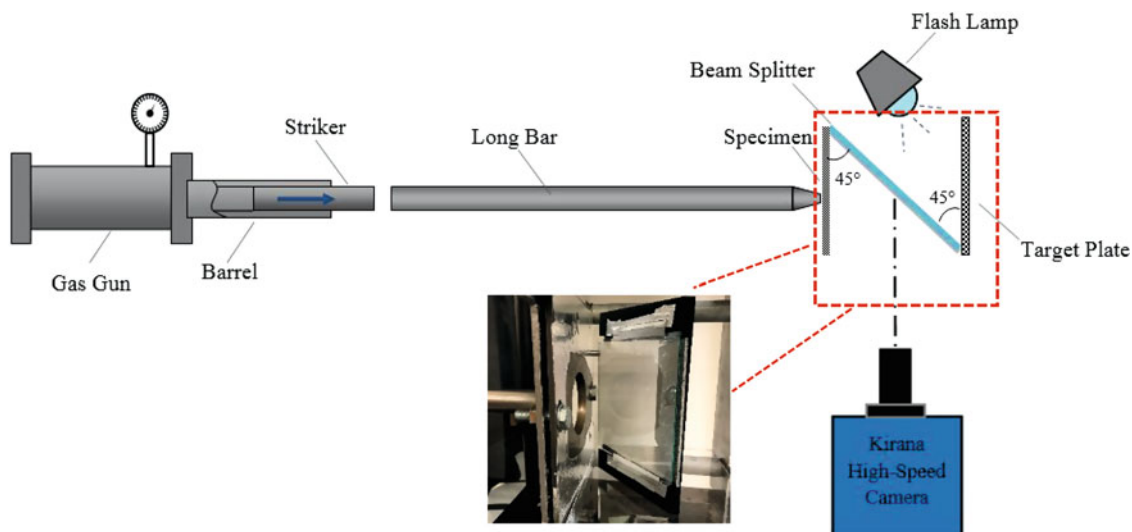
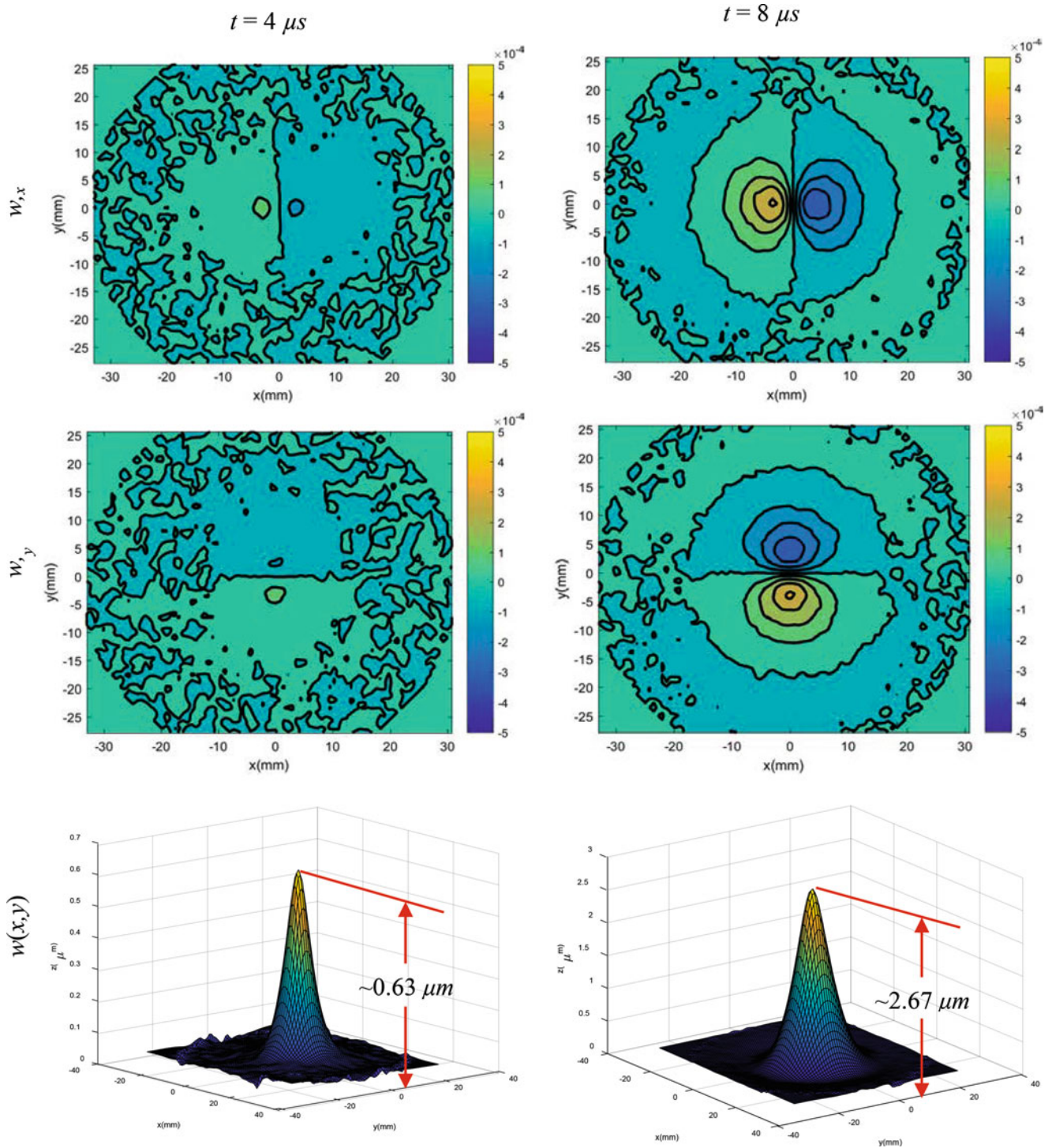
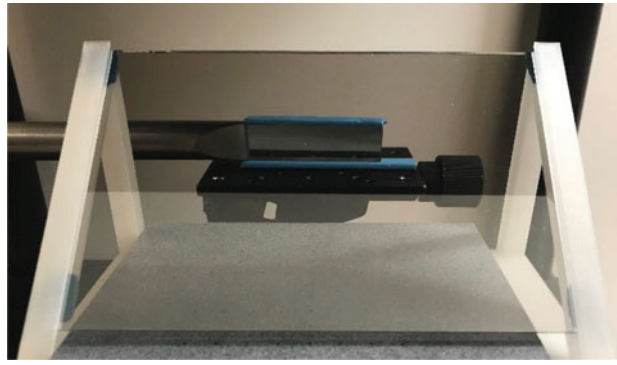


Fig. 57.4 Schematic of the experimental setup for dynamic plate impact study. Inset shows close-up view of the optical arrangement



**Fig. 57.5** Evolution of  $w_{,x}$  (row 1) and  $w_{,y}$  (row 2) contours and surface topography (row 3) for a clamped glass plate subjected to central impact. Note: Location (0, 0) is made to coincide with the loading point. Contour increments =  $8 \times 10^{-5}$  rad

$25.4 \times 6.7 \text{ mm}^2$  rectangular tip. A close-up view of the optical arrangement is shown in Fig. 57.6. As in the previous experiment, a striker was launched towards the long-bar at a velocity of  $\sim 5 \text{ m/s}$  during tests. Simultaneously a Kirana-05 M ultrahigh-speed camera was used to record the speckle on the target plane at 500 K frames per second. The distance between the specimen and the camera lens plane ( $L$ ) was  $\sim 1500 \text{ mm}$  and the one between the specimen mid-plane and the target plane ( $\Delta$ ) was  $177 \text{ mm}$ .



**Fig. 57.6** Close-up view of the optical arrangement for tr-DGS

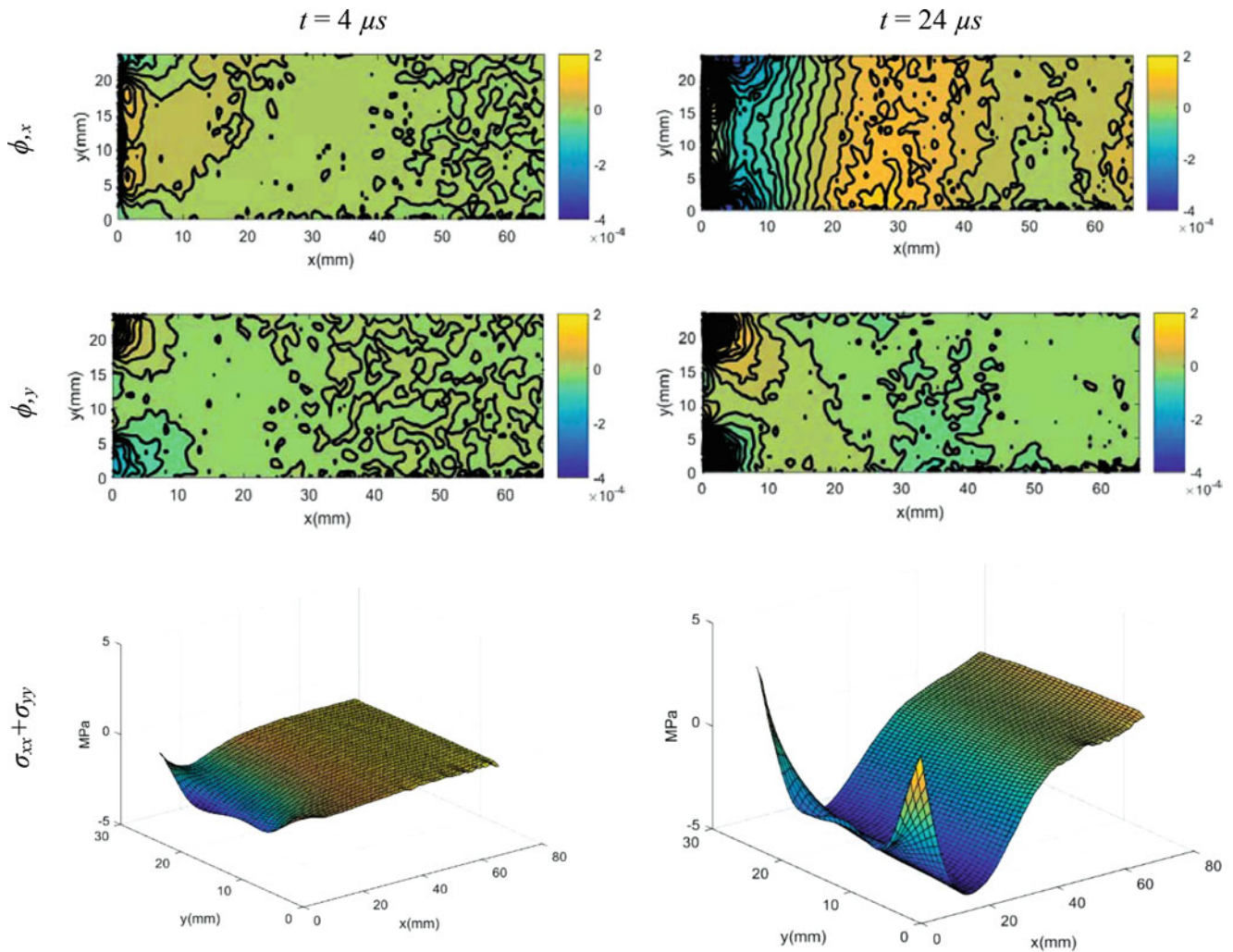


**Fig. 57.7** Evolution of  $\phi_x$  (row 1) and  $\phi_y$  (row 2) contours and stress fields (row 3) for a glass plate subjected to flank side impact. Contour increments =  $2.5 \times 10^{-5}$  rad

The time-resolved orthogonal stress contours  $\phi_{(x:y)}$  due to transient stress wave propagation in the glass plate are shown in the first two rows of Fig. 57.7 at a few select time instants. The start of the impact event is at  $t = 0 \mu s$ . It can be observed that all the contours are symmetric about the center of the sample, confirming a symmetric surface-to-surface contact. The stress concentrations can be observed at the two corners of the specimen. The reconstructed 3D stress fields ( $\sigma_{xx} + \sigma_{yy}$ ) were obtained from the measured stress gradients by using HFLI and are plotted in the 3rd row of Fig. 57.7. The stress concentrations are also very clear in the 3D depiction of the stress fields.

## 57.4 Conclusions

In this paper, two full-field optical methods have been applied to quantitatively visualize out-of-plane deformations and  $(\sigma_{xx} + \sigma_{yy})$  stress fields in thin soda-lime glass subjected to dynamic impact. First, the feasibility of evaluating sub-micron deformations at sub-microsecond temporal resolutions over relatively large regions-of-interest has been demonstrated using r-DGS and HFLI along with ultrahigh-speed photography. Subsequently, another much higher sensitivity method, tr-DGS, has been developed and applied using HFLI to visualize the evolution of  $(\sigma_{xx} + \sigma_{yy})$  stress fields in glass. Thus, both out-of-plane deformations and  $(\sigma_{xx} + \sigma_{yy})$  stress fields are successfully evaluated using variants of DGS methodology.

**Acknowledgement** Support for this research through Army Research Office grants W911NF-16-1-0093 and W911NF-15-1-0357 (DURIP) are gratefully acknowledged.

## References

1. Periasamy, C., Tippur, H.V.: Full-field digital gradient sensing method for evaluating stress gradients in transparent solids. *Appl. Opt.* **51**(12), 2088–2097 (2012)
2. Periasamy, C., Tippur, H.V.: A full-field reflection-mode digital gradient sensing method for measuring orthogonal slopes and curvatures of thin structures. *Meas. Sci. Technol.* **24**, 025202 (2013)
3. Miao, C., Sundaram, B.M., Huang, L., Tippur, H.V.: Surface profile and stress field evaluation using digital gradient sensing method. *Meas. Sci. Technol.* **27**, 095203 (2016)
4. Miao, C., Tippur, H.: Measurement of orthogonal surface gradients and reconstruction of surface topography from digital gradient sensing method. In: *Advancement of Optical Methods in Experimental Mechanics*, pp. 203–206. Springer, Cham (2017)
5. Miao, C., Tippur, H.V.: Measurement of sub-micron deformations and stresses at microsecond intervals in laterally impacted composite plates using digital gradient sensing. *J. Dyn. Behav. Mater.* 1–23 (2018). <https://doi.org/10.1007/s40870-018-0156-4>
6. Miao, C., Tippur, H.V.: Higher sensitivity digital gradient sensing configurations for quantitative visualization of stress gradients in transparent solids. *Opt. Lasers Eng.* **108**, 54–67 (2018)
7. Sundaram, B.M., Tippur, H.V.: Dynamic crack growth Normal to an Interface in bi-layered materials: an experimental study using digital gradient sensing technique. *Exp. Mech.* **56**, 37–57 (2015)
8. Sundaram, B.M., Tippur, H.V.: Dynamics of crack penetration vs. branching at a weak interface: an experimental study. *J. Mech. Phys. Solids.* **96**, 312–332 (2016)
9. Sundaram, B.M., Tippur, H.V.: Dynamic mixed-mode fracture behaviors of PMMA and polycarbonate. *Eng. Fract. Mech.* **176**, 186–212 (2017)
10. Sundaram, B.M., Tippur, H.V.: Dynamic fracture of soda-lime glass: a full-field optical investigation of crack initiation, propagation and branching. *J. Mech. Phys. Solids.* (2018). <https://doi.org/10.1016/j.jmps.2018.04.010>
11. Sundaram, B.M., Tippur, H.V.: Full-field measurement of contact-point and crack-tip deformations in soda-lime glass. Part-I: quasi-static loading. *Int. J. Appl. Glas. Sci.* **9**, 114–122 (2018)
12. Sundaram, B.M., Tippur, H.V.: Full-field measurement of contact-point and crack-tip deformations in soda-lime glass. Part-II: stress wave loading. *Int. J. Appl. Glas. Sci.* **9**, 123–136 (2018)